Compression-bending Behavior of Steel Plate Reinforced Concrete Shear Walls with High Axial Compression Ratio

C. Xiao, C. Tian, T. Chen, D. Jiang
China Academy of Building Research, Beijing

SUMMARY:
The compression-bending behaviour of 12 shear wall specimens with high axial compression ratios were studied by testing under low-frequency cyclic lateral loading. All test specimens were divided into two groups according to different concrete strengths (C50 and C80), and both of them included reinforced concrete (RC) walls and steel plate reinforced concrete (SPRC) walls. Based on the experimental results, the damage pattern, hysteretic characteristics, loading capacity and deformation capacity of specimens were studied. RC walls and SPRC walls had similar failure patterns. Cracks on SPRC walls were narrower. Embedded steel plate in the middle and profiled steels at both ends effectively improved the loading capacity of specimens. Based on test results, SPRC walls' capacity formula and design suggestions were proposed and adopted by the structural design of the Mega Tower of China World Trade Centre to reduce wall thickness for improving building economy.

Keywords: experimental study; compression-bending behaviour; high axial compression ratio; pseudo-static test

1. INTRODUCTION

It is known that reinforced concrete (RC) shear wall is one of the most common lateral resistance members for tall buildings. However, with the increase of the building height, the RC shear walls at the bottom become thicker and less ductile due to much more shear force and gravity load demands, which would be harmful to the structure when it resists earthquake force and decrease the usage space of the building. Therefore, with the development in both structural and architectural demands, composite structure has been more and more widely used in super high-rise buildings' lateral resistance system in recent years.

In the AISC Seismic Provisions (AISC, 1997), the composite shear walls consisting of a steel plate shear wall with reinforced concrete encasement on one or both sides are termed as "Composite Steel Plate Shear Walls (C-SPW)". Compared with traditional RC shear walls, C-SPW has several advantages: 1) C-SPW with the same shear capacity will have smaller thickness and less weight, which provides more useable floor space and results in smaller foundations. 2) The damage to C-SPW can be limited to yielding of steel plates with fewer cracks in the outer concrete or damage to other elements of the system. 3) For C-SPW, the concrete on both sides could provide out-of-plane stiffening to prevent its buckling before it yields. Besides that, the concrete on both sides can provide temperature insulation to steel plate, which saves the costs of fireproofing.

During the past half-century, some researches and engineering applications have been conducted worldwide on composite steel plate shear walls. Composite steel plate shear walls were firstly put into practice in a frame-shear wall dual system of the bus station complex in Japan as early as 1960's (Design Corporation of Japanese Construction, 1964). In US, A. Astaneh-Asl (1998-2002) carried out cyclic loading tests on the composite shear walls which consisted of a steel plate shear wall with RC shear walls attached to one side or both sides of the steel plate using mechanical connectors such as shear studs or bolts. The test results revealed that composite steel plate shear walls are excellent lateral resistance members capable of exceeding inter-story drift values of 4% without reduction in their shear

strength although omission of axial compressive load in test was a regrettable shortcoming. In China, Sun (2007) investigated shear behaviour of composite steel plate shear walls by quasi-static test of 11 specimens with different type of connections. Based on the superposition principle, the design formula of shear strength for composite steel plate shear walls was proposed. During 2008-2009 period, Lu (2009) reported the experimental study on the seismic behaviour of composite steel plate concrete shear walls by low-frequency cyclic loading test on 16 specimens with low concrete strengths (C30 and C50) and the axial compression ratio varied from 0.3 to 0.5. The previous research achievements indicate that for specimens with concrete strength lower than C50, composite steel plate concrete shear walls have better seismic behaviour than ordinary RC shear walls under lower axial compression ratios. However, the research on the composite steel plate shear walls with high concrete strength under high axial compression ratios is much of lackage for engineering practice.

In the paper herein, an experimental study on compression-bending behaviour of an innovative type of composite steel plate shear walls, termed “Steel Plate Reinforced Concrete Shear Wall” (abbr. SPRCW, shown in Fig.1.1), which consists of traditional RC shear wall, steel plate embedded in the middle and profiled steels embedded at both ends, with different concrete strengths (C50 and C80) under high axial compression ratio is described. By carrying out low-frequency cyclic loading tests on 6 specimens, the damage pattern, loading capacity, hysteretic characteristics of SPRCW were studied. In order to investigate the differences in seismic behaviour of SPRC wall and traditional RC wall, the identical tests of 6 traditional reinforced concrete shear wall specimens with same configurations were conducted. Finally based on test results, SPRCW capacity formulas and design suggestions were proposed and adopted by the structural design of Mega Tower of China World Trade Centre.

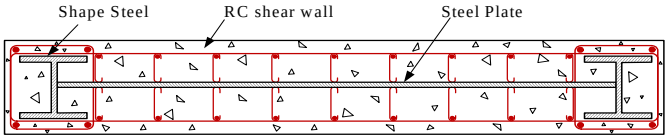

Figure 1.1 Steel plate reinforced concrete shear wall

2. EXPERIMENTAL PROGRAM

2.1. Test Specimens

A total of twelve shear wall specimens were tested under high axial compression ratio, including six reinforced concrete walls (RCW) and six steel plate reinforced concrete walls (SPRCW). Specimens were manufactured by two batches due to different concrete strengths (C50 and C80) and both of them have similar elevations and reinforcement details. The dimensions of all specimens were 2160mm by 800mm. The aspect ratio and the steel percentage in the middle are equal to 2.7 and 3.33%. The wall thickness of C50 specimens is 120mm and its boundary columns have a rectangular cross section of 100×160mm while those two values are 150mm and 100×190mm respectively for C80 specimens. Steel plate and profiled steels were welded together and shear studs were arranged uniformly on the steel plate to guarantee reinforced concrete, steel plate and profiled steels work together. It should be noted that all specimens were designed according to the conception of “strong shear weak bending” to ensure that flexural failure would occur prior to shear failure. Fig.2.1 shows the evaluation and cross-sectional configuration of specimens. The properties of specimens are shown in Table 2.1.

Specimens with different concrete strengths were tested under distinguishing axial compressive loads. All C50 specimens were divided into 3 groups by different axial loads, which were 1070kN, 1290kN and 1510kN. Similarly, three types of axial forces applied on C80 specimens were 2180kN, 2610kN and 3050kN respectively. The steel plate and profiled steels encased in the concrete wall can stand part of the axial compressive load in deed. By taking the contributions of steel plate and profiled steels into consideration, the design axial compression ratios of all specimens were calculated as Eqn.2.1.

and listed in Table 2.1. In Eqn. 2.1, N is axial compressive load, f_c is concrete compression strength, A_c is concrete area, f_a is steel strength, A_a is area of steel plate and profiled steels.

$$n = N/\left(f_c A_c + f_a A_a\right) \tag{2.1}$$

Table 2.1 Properties of Test Specimens

No.	Concrete grade	Wall thickness (mm)	Thickness of the steel plate (mm)	H-shaped profiled steel (mm)	Axial load (kN)	Design Axial compressive ratio
RCW1-a	C50	120	-	-	1070	0.50
RCW2-a	C50	120	-	-	1290	0.60
RCW3-a	C50	120	-	-	1510	0.70
SPRCW1-a	C50	120	4	I50x40x4	1070	0.36
SPRCW2-a	C50	120	4	I50x40x4	1290	0.43
SPRCW3-a	C50	120	4	I50x40x4	1510	0.50
RCW1-b	C80	150	-	-	2180	0.50
RCW2-b	C80	150	-	-	2610	0.60
RCW3-b	C80	150	-	-	3050	0.70
SPRCW1-b	C80	150	5	I50x40x4	2180	0.42
SPRCW2-b	C80	150	5	I50x40x4	2610	0.50
SPRCW3-b	C80	150	5	I50x40x4	3050	0.58

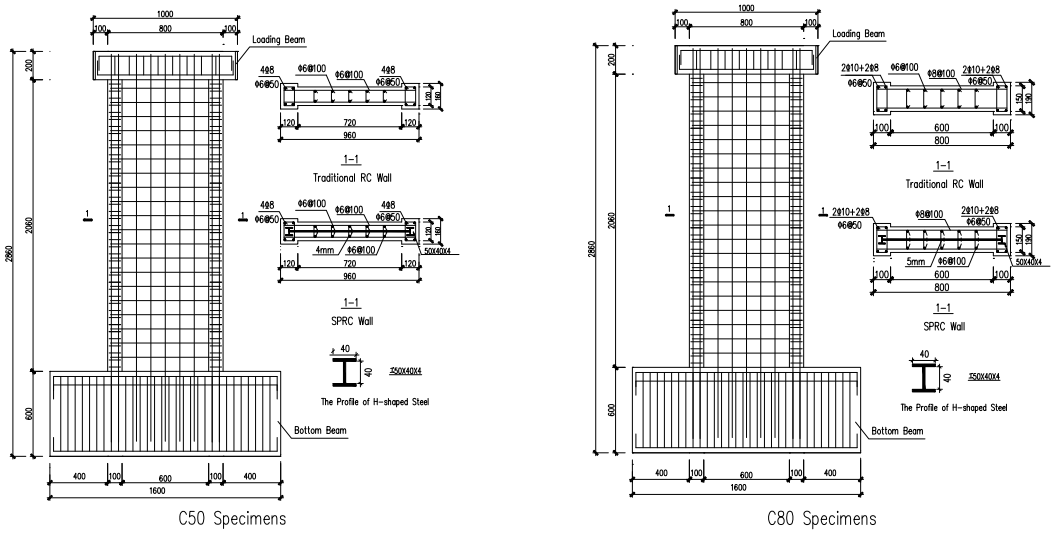

Figure 2.1 Elevations and cross-sectional configuration of test specimens

2.2. Material Properties

The concrete of the specimens was cast-in-situ after formworks completed by two batches according to different concrete strengths (C50 and C80). Especially for C80 specimens, the concrete mix is designed for compressive cube strength, f_{cu}, at 28 days of approximately 80 N/mm^2 before. The C80 concretemix proportions are: P.O 52.5R cement (430 kg/m^3): wollastonite (40 kg/m^3): mineral powder (40 kg/m^3): flyash (60 kg/m^3): sand (820 kg/m^3): coarse aggregate (910 kg/m^3): admixture (14.8 kg/m^3): Water (146 kg/m^3).

The steel Grade was Q345. The H-shaped profiled steels were welded to the steel plates. Cold formed plain bars of 6mm, 8mm and 10mm diameter were applied for the vertical reinforcement and transverse ones. Rebars of 20mm and 25mm diameter were mainly used for the reinforcement of the loading beam and the footing. For each kind of steel and rebar, three test samples were measured and tension tests were carried out on them to determine their dimensions and the material properties. The

properties of concrete, reinforcement bars and steel plate are shown in Table 2.2.

Table 2.2 Properties of Concrete, Reinforcement Bars and Steel Plate

Specimen batches	Concrete		Reinforcement bar and steel plate			
	Cubic strength f_{cu} (Mpa)	Prism Strength f_c (Mpa)	Steel type	Measured Dimension (mm)	f_y （MPa）	f_u （MPa）
C50	47.7	36.3	Φ 6	6.5	368.6	468.9
			Φ 8	8.4	245.2	383.1
			4mm*	3.5*	353.4	469.1
C80	84.1	59.7	Φ 6	6.8	298.3	407.1
			Φ 8	8.3	291.2	431.5
			Φ 8	8.3	446.3	593.7
			Φ 10	10.2	436.1	595.3
			4mm*	3.6*	334.0	454.9
			5mm*	4.7*	309.5	415.0

NOTE: * refers to steel plate

2.3. Test Set-up and Test Regime

The pseudo-static experiment was carried out in The Structural Laboratory of CABR(China Academy of Building Research). All of the twelve specimens were tested under constant axial compressive loads and cyclic horizontal forces. The test setup is displayed in Fig.2.2. Main components of the test setup are gantry, hydraulic jack, distribution beam, sliding plate and reaction wall. The specimen is fixed to the test floor through 4 post-tensioned anchor rods in order to establish a well-defined boundary condition at the foundation. The gantry was adopted in the vertical loading and the constant vertical axial load was provided on the top surface of the loading beam by a vertical hydraulic jack. The lateral load was applied by the horizontal hydraulic actuator which was fixed on the reaction wall and transferred from the top loading beam to both concrete component of the SPRCW and the internal steel plate. One lubricated sliding plate was placed between the gantry and the jack to ensure no lateral restraint existed in the loading process. Lateral braces were settled at each side of the specimen to prevent potential out-plane torsion failure during the test.

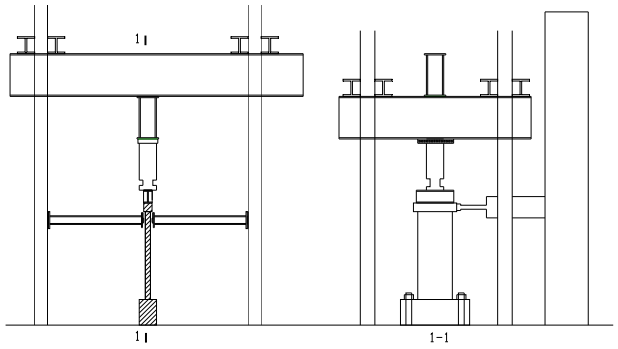

Figure 2.2 Test set-up

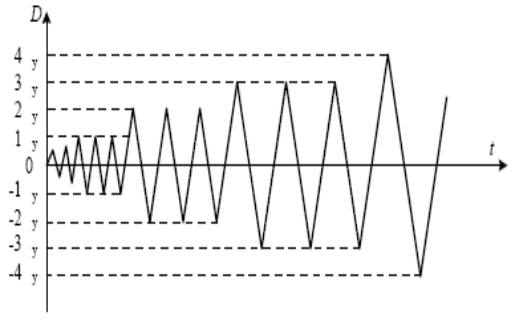

Figure 2.3 Loading sequence

Throughout the experiment, both of the global deformation at the top of the specimen and local strains at the critical locations of reinforcement bars and steel sections were measured. The horizontal force applied on the specimen was measured by the load cell in the actuator. The horizontal displacement on the top of the shear wall was measured by the displacement gauge and recorded by computer. At the same time, lateral force-displacement curve was plotted automatically to monitor the test procedure.

After several small cycles of loading to check the instrumentation, the main test proceeded. The loading sequence of main test for each specimen could be divided into three steps: in the first step, compression force was applied on specimens and kept constant during the following steps. The second step was applying cyclic horizontal forces with loading increase control as 40kN, 60kN, 80kN, 100kN

(C80 specimens: 100kN, 200kN, 300kN, 350kN) and so on until the tensioned longitudinal rebar in boundary element reached its yield strain. Then test regime changed into displacement control by taking the displacement at longitudinal rebar yielded as increasing interval and continued the cyclic loading with repeating twice for each interval until the shear force reduced below 85% of maximum load or the specimen was failure. The loading sequence applied to the specimens is shown in Fig.2.3.

3. EXPERIMENTAL RESULTS

3.1. Behaviour of Specimens

For specimens with different concrete strength (C50 and C80), RCW and SPRCW test specimens showed the similar behavior during the test procedure, which can be summarized into four phases. In the following, a brief summary of the behavior of specimens is provided.

1) Elastic phase.
From cyclic loading beginning to boundary element at tension side cracking, the concrete was still in elastic working state due to the vertical compression load. The relationship between lateral force and displacement kept linear.

2) Cracking phase. Thin visible transverse cracks due to flexure emerged at the bottom of the boundary element at tension side when lateral force reached about 120kN to 180kN (C80 specimens: 300kN to 450kN). More new transverse cracks appeared and spread upwards along the boundary element with the increase of lateral load. The flexural cracks were also found on the surface of wall. In the view of RCW specimens, a few transverse cracks grew into diagonal cracks caused by shear. However, much more transverse cracks grew into diagonal cracks in SPRCW specimens.

3) Yielding phase. In the early stage, more cracks appeared on boundary elements, especially longitudinal cracks appeared on the boundary element of the compression side and the cover concrete became crushed. More transverse and diagonal cracks appeared on the wall surface as well. With regard to RCW specimens, the flexural transverse cracks and few shear diagonal cracks spread to the middle of the wall. For SPRCW specimens, shear diagonal cracks developed so quickly. In this midterm of this phase, all cracks intersected with each other and formed a retiform distribution. After that, no more new cracks appeared in the specimens. The existing cracks on the boundary elements developed deeply as well as a few cracks of wall. And the width of cracks in boundary elements and wall increased much, which was even over 2mm at the bottom of the specimen. The concrete at the foot of boundary element crushed seriously. The specimen reached the peak value of its shear strength.

4) Failure phase. After reaching the peak value, the horizontal loading capacity of the specimen began to decrease as displacement loading increasing. The width of the cracks at the bottom of specimen increased heavily. The concrete at the bottom of boundary element crushed totally and local concrete of wall in compression side also split. The horizontal loading capacity of specimen reduced below 85% of peak value at last.

In summary, typical flexural failure was shown in all specimens. To some extent, SPRCW specimens showed a certain shear failure mode with more obvious shear diagonal cracks than RCW specimens.

3.2. Damage Patterns

RCW and SPRCW specimens with different concrete strength (C50 and C80) shared the similar damage pattern in the experiment. Fig.3.1 shows the final crack distributions of traditional RCW and SPRCW test specimens (C50 and C80) under different axial compressive loads. In the figure, it is shown that cracks are mainly distributed at the middle-lower part of boundary element and wall. Under the same axial compressive load, SPRCW specimens have more cracks than RCW specimens but more intensive and thinner. In the view of same type specimen, the cracks developed less as the

axial compressive ratio increase, which reveals that axial compression can make cracks close up.

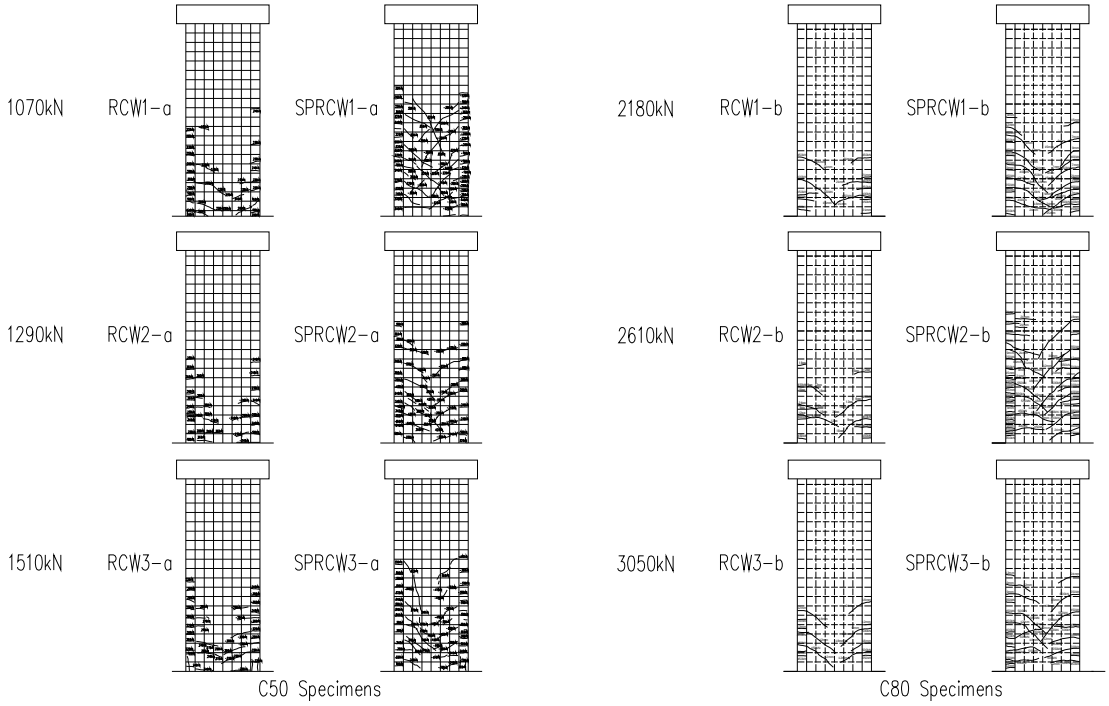

Figure 3.1 Final crack distributions of specimens

3.3. Hysteretic Characteristics

Extensive data were collected from the acquisition system recorders during these tests. One of the most important results is the relationship curve for lateral force versus displacement. Hysteretic characteristics and deformability of specimens can be given from these plots. Fig.3.2 ~3.3 shows the lateral force-displacement hysteretic loops of specimens with concrete strength of C50 and C80.

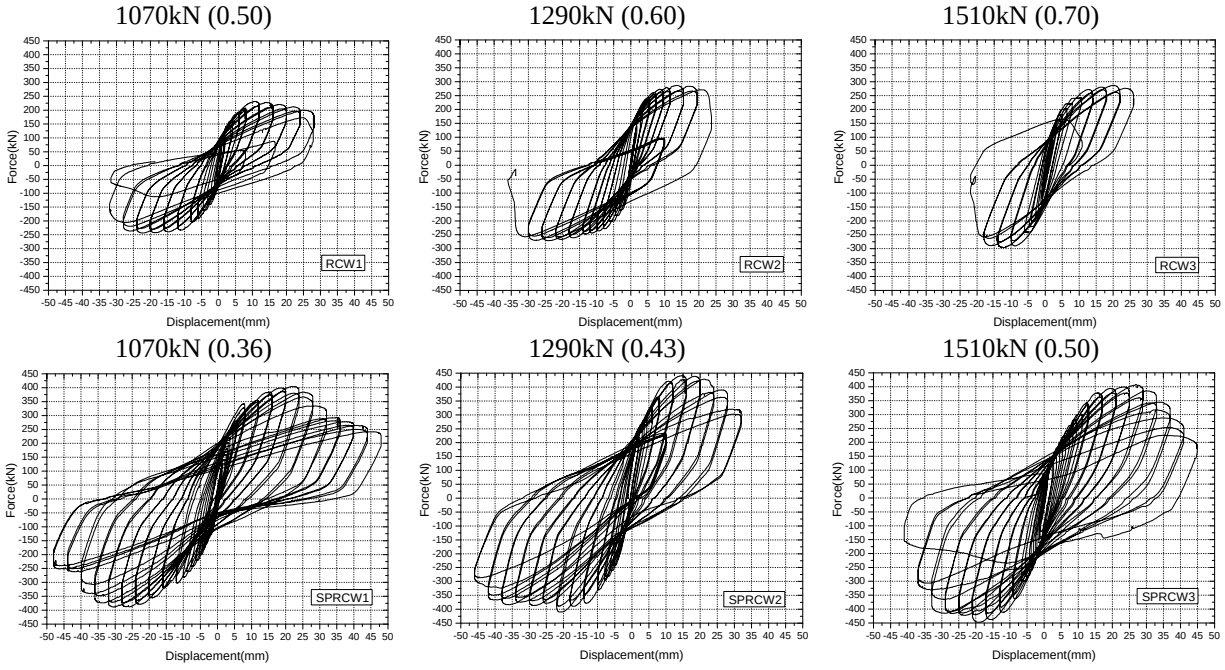

Figure 3.2 Lateral force-displacement hysteretic loops of C50 specimens

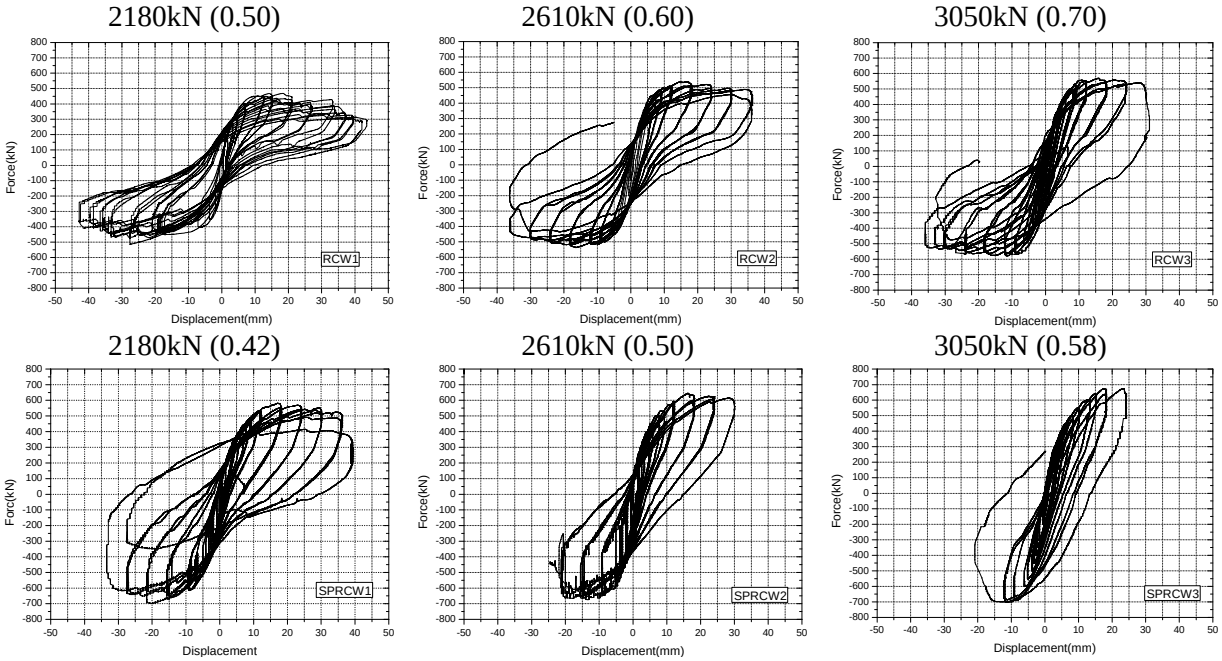

Figure 3.3 Lateral force-displacement hysteretic loops of C80 specimens

From Fig.3.2~3.3, it reveals that: 1) The axial compressive load has significant influence upon the hysteretic curve. The hysteretic curves of test specimens are less stable under higher axial compressive load. 2) For specimens with certain concrete strength, compared with RCW, SPRCW has larger lateral loading capacity, stronger deformation capacity, bigger area enclosed by hysteretic curve. 3) Compared with C50 specimens under similar compressive ratio, C80 ones have larger lateral loading capacity but smaller deformation capacity and area enclosed by hysteretic curve.

3.4. Loading Capacity and Deformation Capacity

Another important experimental result is skeleton curve which can be obtained by means of enveloping lateral force-displacement curve. Quite a lot of valuable information for evaluating seismic behaviour of the specimens can be given from these plots, such as loading capacity and ductility, and all key characteristics are very important in design and analysis of structures.

3.4.1. Loading capacity

For lateral resistance member, the maximal lateral force in the skeleton curve reflects its ultimate capacity to resist horizontal load such as: earthquake and wind. The cracking load is the indicator of the structural members' service performance, which is very important to show whether the building can continue its full functionality. In the experiment, cracking load was recorded when the first visible crack appeared. Fig.3.4 shows the relationships of axial compressive load and ultimate loading capacity. Cracking load, yield load and ultimate capacity of test specimens are listed in Table 3.1.

Table 3.1 Cracking Load, Yield Load and Ultimate Capacity of Specimens

Specimen batches	No.	Cracking load (kN)		Yielding load (kN)			Ultimate capacity (kN)		
		+	-	+	-	Average	+	-	Average
C50	RCW1-a	350	350	393.7	417.7	405.7	468.6	514.2	491.4
	RCW2-a	400	400	464.4	448.3	456.4	540.3	536.3	538.3
	RCW3-a	400	450	490.4	487.2	488.8	569.7	578.2	574.0
	SPRCW1-a	300	300	492.5	592.5	542.5	580.6	696.9	638.8
	SPRCW2-a	300	300	535.7	574.7	555.2	645.5	673.8	659.7
	SPRCW3-a	450	450	560.4	581.0	570.7	674.2	701.1	687.7
C80	RCW1-b	140	140	183.5	185.9	184.7	231.6	243.3	237.5
	RCW2-b	180	180	239.9	204.5	222.2	286.9	270.8	278.9

	RCW3-b	160	160	220.7	245.8	233.3	286.8	296.0	291.4
	SPRCW1-b	140	140	295.8	257.7	276.8	404.5	388.3	396.4
	SPRCW2-b	180	180	332.1	287.7	309.9	441.4	409.8	425.6
	SPRCW3-b	120	120	273.5	316.5	295.0	407.9	447.2	427.6

NOTE: '+' refers push direction and '-' refers pull direction

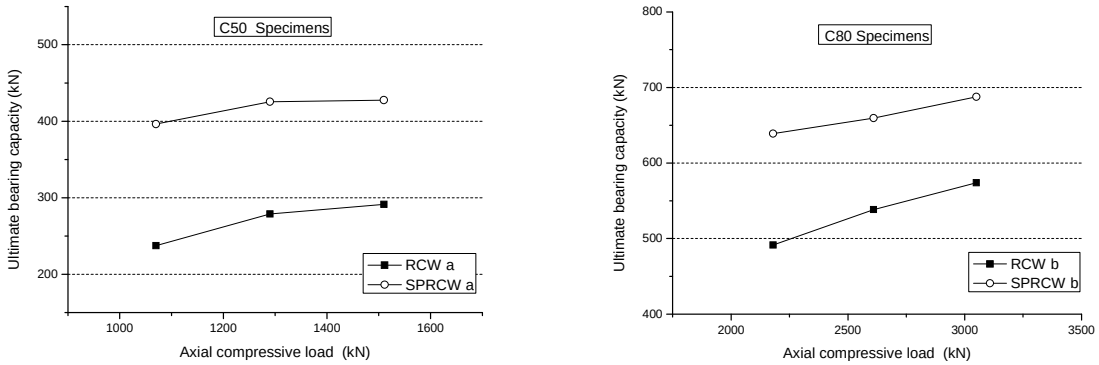

Figure 3.4 Loading capacity-axial compressive load of test specimens

From Table 3.1 and Figure 3.4, it reveals that: 1) Under the same axial compressive load, SPRCW specimens can provide more load capacities (20%~30% of ultimate lateral loads) than RCW specimens. 2) For the same type of specimens, the ultimate lateral load capacities also improved partially with the increase of the axial compressive load. 3) For test specimens with the same concrete strength, first visible crack appeared earlier in SPRCW specimens than RCW ones. 4) For the same type of specimens, the ultimate loading capacity of C80 specimens is much larger compared with that of C50 ones under similar axial compressive ratio.

3.4.2. Deformation capacity

For lateral resistance member, deformation capacity is another critical aspect to evaluate its seismic behaviour and it can be indicated by several indexes such as ductility, maximal drift and so on. Ductility index, termed as $\mu = \Delta_u / \Delta_y$, was adopted in this paper. By taking the contributions of steel plate and profiled steels into consideration in design axial compressive ratio calculation (Equation 2.1), we get the design axial compressive ratios of test specimens.

Fig.3.5~3.6 shows the relationships of ductility index versus axial compressive load and ratio. Ductility index of test specimens are listed in Table 3.2. From Figure 3.5~3.6 and Table 3.2, it reveals that: 1) As the axial compressive load/ratio increasing to a certain extent, the ductility index of test specimens decreases significantly. 2) For SPRCW, C50 specimens show better deformation capacity compared with C80 specimens. 3) Especially for C80 SPRCW specimens, the ductility value has fallen below 3 when the compressive ratio exceeds 0.6. And the structural member cannot be put into practice in this condition.

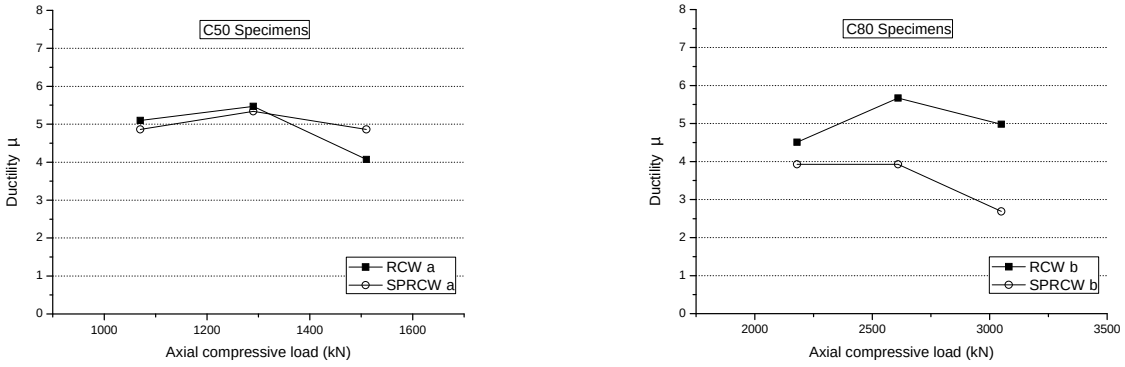

Figure 3.5 Ductility-axial compressive load of test specimens

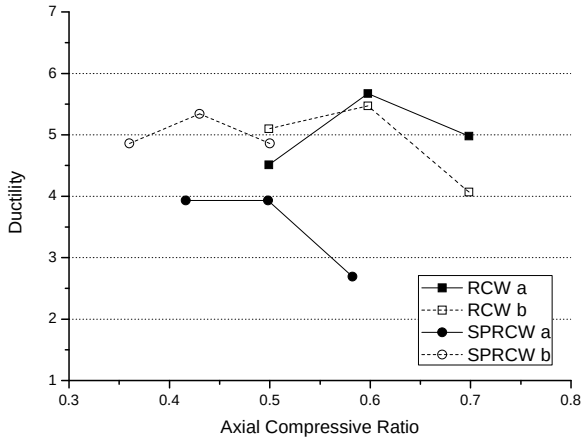

Figure 3.6 Ductility-axial compressive ratio

Table 3.2 Ductility of Specimens

No.	Axial Load	n	Ductility		
			+	-	Aver.
RCW1-a	1070kN	0.50	5.00	5.20	5.10
RCW2-a	1290kN	0.60	4.61	6.33	5.47
RCW3-a	1510kN	0.70	4.10	4.03	4.07
SPRCW1-a	1070kN	0.36	4.78	4.93	4.86
SPRCW2-a	1290kN	0.43	4.83	5.85	5.34
SPRCW3-a	1510kN	0.50	4.29	5.40	4.86
RCW1-b	2180kN	0.50	5.19	3.84	4.51
RCW2-b	2610kN	0.60	4.84	6.49	5.67
RCW3-b	3050kN	0.70	3.92	6.03	4.98
SPRCW1-b	2180kN	0.42	3.91	3.95	3.93
SPRCW2-b	2610kN	0.50	3.62	4.24	3.93
SPRCW3-b	3050kN	0.58	2.24	3.15	2.69

NOTE: '+' refers push direction and '-' refers pull direction

4. FORMULA FOR SPRCW FLEXURAL CALCULATION

The strain distributions at the peak value of lateral load of SPRCW specimens with different concrete strengths (shown in Fig.4.1), recorded by the gauges arranged on the steel plate in the length direction of profile, validate that the plane section assumption can still be kept. So based on the plane section assumption, the formula for SPRCW flexural calculation can be derived as Fig.4.2 shows and expressed in Equation 4.1.

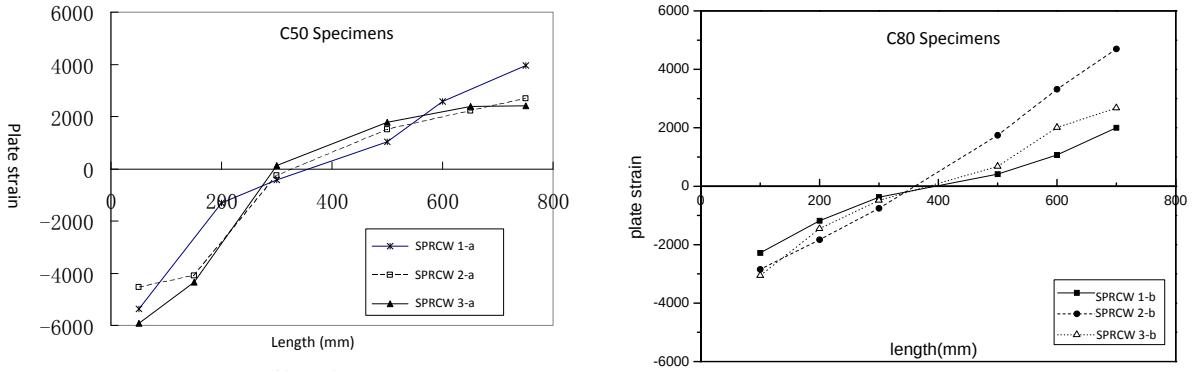

Figure 4.1 Strain distribution of steel plate at bottom section

$$\begin{cases} N \le \dfrac{1}{\gamma_{RE}}[N_c + f_a' A_a' + f_y' A_s' - \sigma_a A_a - \sigma_s A_s + N_{sw} + N_{pw}] \\ Ne \le \dfrac{1}{\gamma_{RE}}[M_c + f_a' A_a' (h_0 - a_a') + f_y' A_s' (h_0 - a_s') + M_{sw} + M_{pw}] \end{cases} \tag{4.1}$$

In Eqn. 4.1, $N_{pw} = (1 + \dfrac{\xi - \beta_1}{0.5\beta_1\omega_p}) f_{pw} A_{pw}$, $M_{pw} = [0.5 - (\dfrac{\xi - \beta_1}{\beta_1\omega_p})^2] f_{pw} A_{pw} h_{pw}$, A_{pw}, f_{pw} are the cross area and design strength of the steel plate encased in concrete wall. β_1 is a parameter related to the concrete strength grade. N_{pw} is the axial force taken by steel plate. M_{pw} is the moment of resultant force of steel plate to centre of shape steel. When $\xi > \beta_1$, $N_{pw} = f_{pw} A_{pw}$. $M_{pw} = 0.5 f_{pw} A_{pw} h_{pw}$ when $\xi > 0.8$. ω_a is the ratio of steel plate height h_{pw} to section effective height h_0. Other notations are listed in *Chinese Code -Technical specification for steel reinforced concrete composite structures*.

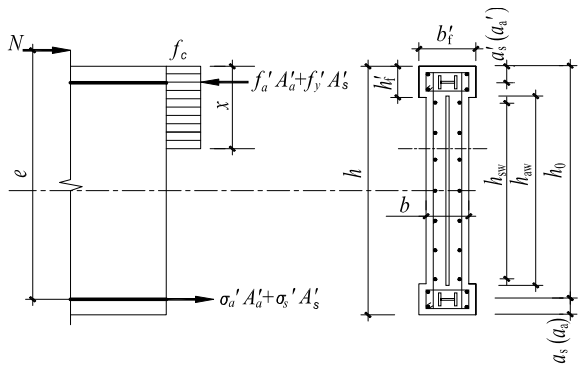

Figure 4.1 Analytical model of section

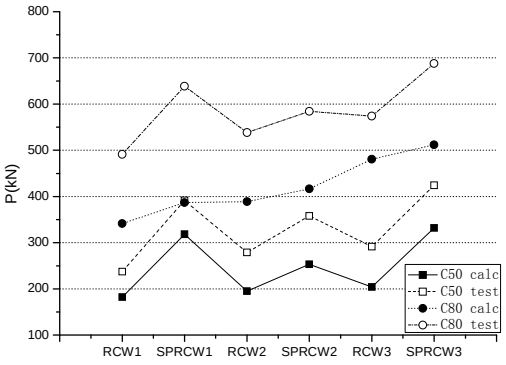

Figure 4.2 Calculation and test results

The comparison of the maximum lateral load value of test and calculation (shown in Fig.4.2) shows the formula proposed has good coherence and certain reliability. The proposed formula was adopted in the structural design of the Mega Tower of China World Trade Centre. They addressed that the SPRCW provides one effective way to keep enough ductility and improve the load capacity for shear wall at meantime.

5. CONCLUSIONS

The compression-bending behaviour of the steel plate reinforced concrete shear wall is investigated by low-frequency cyclic loading tests on a series of test specimens. Through the experiment, damage pattern, loading capacity and deformation capacity were studied. Finally, design formula for SPRCW flexural calculation was proposed based the assumption of plane section. The following conclusions can be derived from this study: 1) SPRCW specimens have lighter damage and better hysteretic characteristics than those of traditional RCW ones under the same axial compressive load. 2) For specimens with similar axial compressive ratio, SPRCW can provide 20%~30% more lateral load capacity and better ductility compared with RCW. For the same type of specimens, the ultimate loading capacity of C80 specimens is much larger compared with that of C50 ones .3) As the axial compressive load/ratio increasing, the ultimate loading capacity will increase but the ductility index of test specimens decreases significantly when it increases to a certain extent. Especially for C80 SPRCW specimens, the ductility value has fallen below 3 when the compressive ratio exceeded 0.6. 5) The formula proposed for calculating SPRCW flexural capacity has good coherence with test results and certain reliability.

5. REFERENCES

The American Institute of Steel Construction (AISC) (1997). Seismic Provisions for Structural Steel Buildings, the United States.

Association of Japanese Building Technicians (2005).100 Examples for Structural Techniques in Japan. Chinese Building Industry Press, Beijing.

Qiuhong Zhao, Abolhassan Astaneh-Asl. (2004). Cyclic Behavior of Traditional and Innovative Composite Shear Walls. *Journal of Structural Engineering- ASCE.* **130:2**, 271-284.

Tao Chen. (2011). Experimental study of the compression-bending behavior of composite shear walls of high axial compression ratios. *China Civil Engineering Journa.* **44:6**, 1-8.

Dongqi Jiang. (2012). Experimental study of the compression-bending behaviour of high-strength concrete steel composite shear walls. *China Civil Engineering Journa.* **45:3**, 17-25.

Jianchao Sun. (2008). Experimental study on shear behavior of steel plate-concrete composite wall. *building Structure.* **38:6**, 1-5.

C.J. Gan, X.L. Lu and W. Wang. (2008). Seismic Behavior of Steel Plate Reinforced Concrete Shear Walls. *The 14th World Conference on Earthquake Engineering.*

X.L. Lu, Y.G. Dong, Z.W. Ding. (2006). Study on seismic behavior of steel reinforced concrete wall. *Earthquake Engineering And Engineering Vibration.* **26:6**, 101-107.